Efficient Simulation of Multiple Cross-Correlated Rayleigh Fading Channels

Cheng-Xiang Wang and Matthias Pätzold
Department of Information and Communication Technology
Faculty of Engineering and Science, Agder University College
Grooseveien 36, N-4876 Grimstad, Norway
E-mail: cheng.wang@hia.no

Abstract – **For the simulation of practical diversity combined fading channels, multiple-input multiple-output (MIMO) channels, and space-time-selective fading channels, it is desirable to produce multiple Rayleigh fading processes with specified cross-correlations. Based on the deterministic sum-of-sinusoids (SOS) channel modeling approach, we have developed a simple efficient procedure for generating an arbitrary number of cross-correlated Rayleigh fading processes. It is demonstrated by numerical and simulation results that the resulting deterministic channel simulator can accurately reproduce all of the desired statistical properties, such as the autocorrelation functions (ACFs), the cross-correlation functions (CCFs), and the phase properties.**

I. Introduction

Multiple correlated Rayleigh fading signals are commonly encountered in wireless communication systems, such as MIMO systems, space-time-selective systems, diversity systems, and multicarrier code-division multiple access (MC-CDMA) systems. For convenience, researchers simulating these systems have typically assumed that the received signal envelopes are uncorrelated. However, the fadings experienced by different diversity branches are often correlated due to restricted antenna spacing in space diversity systems and insufficient frequency separation in frequency diversity systems. Also, significant correlations may exist among subcarrier fades when the number of carriers notably exceeds the degree of system diversity in practical MC-CDMA systems. Therefore, efficient and accurate computer simulations of multiple cross-correlated Rayleigh fading channels are of great importance for realistic performance assessments of those systems.

In the literature, different methods have been presented for the generation of two [1, 2] or any number [3–8] of correlated Rayleigh fading processes. Among them, channel simulators based on the filter method [5], the inverse discrete Fourier transform (IDFT) method [6, 7], and the autoregressive (AR) method [8] have become popular. However, the filter method does not provide precise matching of the desired statistics. The IDFT method requires a large storage for the generation of a large number of random variants. The stochastic AR models are known to be high quality fading channel simulators, while they have to pay relatively high computational efforts. The deterministic SOS channel modeling approach [9–12] is an established method for simulating Rayleigh fading channels. To the best of authors' knowledge, how to use the deterministic SOS method to generate an arbitrary number of correlated Rayleigh fading processes has not been reported in the literature to date.

In the present study, a generic procedure for producing multiple cross-correlated Rayleigh fading envelopes will be described. For this purpose, multiple uncorrelated fading processes with given ACFs are first generated by properly choosing the discrete Doppler frequencies of the deterministic SOS channel simulator. Then, a linear transformation (LT) is applied to produce the desired multiple fading processes with specified CCFs. The simulated correlated fading envelopes, the corresponding phase processes, the ACFs, and the CCFs will be illustrated. Compared with other fading channel simulators, our model stands out with the ability of both accurate reproduction of all of the desired statistical properties and efficient implementation due to the retained deterministic nature.

The remainder of this paper is organized as follows. In Section II, a design method for the generation of correlated Rayleigh fading processes is described. A corresponding simulation model based on the deterministic SOS channel modeling approach is presented in Section III. Section IV gives some simulation results and discussions. Finally, the conclusions are drawn in Section V.

II. Design Method

It is well known that a Rayleigh process is obtained by taking the absolute value of a zero-mean complex Gaussian random process. Our goal is to generate $\mathcal{L}$ complex Gaussian random processes with specified ACFs and any desired cross-correlations. The idea is simply to factorize the given correlation matrix, followed by a LT of $\mathcal{L}$ uncorrelated complex Gaussian random processes [4, 13].

Let us denote the desired ℓth ($\ell = 1, 2, \ldots, \mathcal{L}$) Rayleigh

0-7803-7822-9/03/$17.00 © 2003 IEEE.

fading process by $z_\ell(t)$, which is given by

$$z_\ell(t) = |y_\ell(t)| = |y_{1,\ell}(t) + jy_{2,\ell}(t)| \,. \tag{1}$$

Here, $y_\ell(t)$ is a complex Gaussian random process with mean zero, its inphase component $y_{1,\ell}(t)$ and quadrature component $y_{2,\ell}(t)$ are independent real Gaussian noise processes with identical variances σ_0^2 and ACFs. A widely accepted reference model assumes that the plane waves propagate in a two-dimensional (2-D) environment and arrive at the omnidirectional receive antenna from all directions with equal probability. This model is commonly referred to as Clarke's 2-D isotropic scattering model [11, 14]. In this case, the Doppler power spectral density (PSD) of the scattered components $y_\ell(t)$ has the well-known U-shaped bandlimited form

$$S_{y_\ell y_\ell}(f) = \begin{cases} \frac{2\sigma_0^2}{\pi f_{max}\sqrt{1-(f/f_{max})^2}} \,, & |f| \le f_{max} \\ 0 \,, & |f| > f_{max} \end{cases} \tag{2}$$

where f_{max} is the maximum Doppler frequency. The inverse Fourier transform of $S_{y_\ell y_\ell}(f)$ results in the corresponding ACF $r_{y_\ell y_\ell}(\tau)$ of $y_\ell(t)$

$$r_{y_\ell y_\ell}(\tau) = 2\sigma_0^2 J_0(2\pi f_{max}\tau) \tag{3}$$

where $J_0(\cdot)$ denotes the zeroth-order Bessel function of the first kind.

Now, suppose that the desired correlation matrix $\mathbf{W}$ of the complex Gaussian random processes $y_\ell(t)$ ($\ell = 1, 2, \ldots, \mathcal{L}$) is given by

$$\mathbf{W} = \begin{bmatrix} \rho_{11} & \rho_{12} & \cdots & \rho_{1\mathcal{L}} \\ \rho_{21} & \rho_{22} & \cdots & \rho_{2\mathcal{L}} \\ \vdots & \vdots & \ddots & \vdots \\ \rho_{\mathcal{L}1} & \rho_{\mathcal{L}2} & \cdots & \rho_{\mathcal{L}\mathcal{L}} \end{bmatrix} . \tag{4}$$

In (4), each entry $\rho_{\ell\lambda}$ ($\ell, \lambda = 1, 2, \ldots, \mathcal{L}$) of the matrix $\mathbf{W}$ is called the correlation coefficient (the normalized correlation function at the origin) between the complex Gaussian random processes $y_\ell(t)$ and $y_\lambda(t)$, i.e.,

$$\rho_{\ell\lambda} = \frac{r_{y_\ell y_\lambda}(\tau)}{\sqrt{r_{y_\ell y_\ell}(\tau) r_{y_\lambda y_\lambda}(\tau)}} \Big|_{\tau=0} \,. \tag{5}$$

Apparently, $\rho_{\ell\ell} = 1$ and $\rho_{\ell\lambda} = \rho_{\lambda\ell}$ hold for all $\ell, \lambda = 1, 2, \ldots, \mathcal{L}$. Consequently, $\mathbf{W} = \mathbf{W}^T$ holds, where T indicates the matrix transpose. Therefore, $\mathbf{W}$ is a symmetric matrix with unit diagonal values.

Next, a generic procedure will be provided to enable the generation of the above $\mathcal{L}$ correlated complex Gaussian random processes $y_\ell(t)$ ($\ell = 1, 2, \ldots, \mathcal{L}$). To this end, we could start by generating $\mathcal{L}$ independent complex Gaussian random processes with the ACFs given by (3). Then, these uncorrelated processes will be combined in a weighting network (or a coloring matrix) to achieve the desired correlated processes.

Let us denote the $\mathcal{L}$ statistically independent complex Gaussian random processes as $\mu_\ell(t)$ ($\ell = 1, 2, \ldots, \mathcal{L}$). The inphase component $\mu_{1,\ell}(t)$ and quadrature component $\mu_{2,\ell}(t)$ have zero mean and common variance σ_0^2. It follows that the magnitude of the complex Gaussian random process $\zeta_\ell(t) = |\mu_\ell(t)|$ has a Rayleigh distribution. The ACF of $\mu_\ell(t)$ is given by

$$r_{\mu_\ell\mu_\ell}(\tau) = 2\sigma_0^2 J_0(2\pi f_{max}\tau) \tag{6}$$

while the CCF between $\mu_\ell(t)$ and $\mu_\lambda(t)$ is $r_{\mu_\ell\mu_\lambda}(\tau) = 0$ for $\ell \neq \lambda$ and $\ell, \lambda = 1, 2, \ldots, \mathcal{L}$. Then, the desired cross-correlated complex Gaussian random processes $y_\ell(t)$ can be generated as a linear combination of $\mu_\ell(t)$ [13]

$$\begin{aligned} y_1(t) &= c_{11}\mu_1(t) + c_{12}\mu_2(t) + \cdots + c_{1\mathcal{L}}\mu_\mathcal{L}(t) \\ y_2(t) &= c_{21}\mu_1(t) + c_{22}\mu_2(t) + \cdots + c_{2\mathcal{L}}\mu_\mathcal{L}(t) \\ &\vdots \\ y_\mathcal{L}(t) &= c_{\mathcal{L}1}\mu_1(t) + c_{\mathcal{L}2}\mu_2(t) + \cdots + c_{\mathcal{L}\mathcal{L}}\mu_\mathcal{L}(t) \end{aligned} \tag{7}$$

where the quantities $c_{\ell k}$ ($\ell, k = 1, 2, \ldots, \mathcal{L}$) are real values. In matrix form, (7) can be rewritten as

$$\mathbf{Y} = \mathbf{C}\mathbf{U} \tag{8}$$

where $\mathbf{Y} = [y_1(t) \;\; y_2(t) \;\; \cdots \;\; y_\mathcal{L}(t)]^T$, $\mathbf{U} = [\mu_1(t) \; \mu_2(t) \; \cdots \; \mu_\mathcal{L}(t)]^T$, and

$$\mathbf{C} = \begin{bmatrix} c_{11} & c_{12} & \cdots & c_{1\mathcal{L}} \\ c_{21} & c_{22} & \cdots & c_{2\mathcal{L}} \\ \vdots & \vdots & \ddots & \vdots \\ c_{\mathcal{L}1} & c_{\mathcal{L}2} & \cdots & c_{\mathcal{L}\mathcal{L}} \end{bmatrix} \tag{9}$$

is called the coloring matrix. It follows from (7) that the ACF of $y_\ell(t)$ is computed by

$$r_{y_\ell y_\ell}(\tau) = \sum_{k=1}^{\mathcal{L}} c_{\ell k}^2 r_{\mu_k\mu_k}(\tau) \,. \tag{10}$$

Since the ACFs $r_{\mu_k\mu_k}(\tau)$ are identical for all $k = 1, 2, \ldots, \mathcal{L}$ [see (6)],

$$r_{y_\ell y_\ell}(\tau) = r_{\mu_\ell\mu_\ell}(\tau) \sum_{k=1}^{\mathcal{L}} c_{\ell k}^2 \tag{11}$$

holds. Under the assumption that $r_{y_\ell y_\ell}(\tau) = r_{\mu_\ell\mu_\ell}(\tau)$ [see (3) and (6)] holds, each row of the matrix $\mathbf{C}$ has to fulfill the following condition

$$\sum_{k=1}^{\mathcal{L}} c_{\ell k}^2 = 1 \,, \quad \ell = 1, 2, \ldots, \mathcal{L} \,. \tag{12}$$

From (7), it can also easily be shown that the CCF between $y_\ell(t)$ and $y_\lambda(t)$ for $\ell \neq \lambda$ ($\ell, \lambda = 1, 2, \ldots, \mathcal{L}$) can be expressed as

$$r_{y_\ell y_\lambda}(\tau) = r_{\mu_\ell\mu_\ell}(\tau) \sum_{k=1}^{\mathcal{L}} c_{\ell k} c_{\lambda k} \,. \tag{13}$$

The expression (13) clearly indicates that the CCFs of any pair of cross-correlated Gaussian random processes $y_\ell(t)$ generated by the above approach are restricted to have the same shape as the ACFs of the underlying independent Gaussian processes $\mu_\ell(t)$. According to (5), the cross-correlation coefficient $\rho_{\ell\lambda}$ between $y_\ell(t)$ and $y_\lambda(t)$ is given by

$$\rho_{\ell\lambda} = \sum_{k=1}^{\mathcal{L}} c_{\ell k} c_{\lambda k} \ . \tag{14}$$

From (12) and (14), the following matrix form expression can be obtained

$$\mathbf{W} = \mathbf{C}\mathbf{C}^T \ . \tag{15}$$

The confronted problem now is to find the coloring matrix $\mathbf{C}$ given the symmetric correlation matrix $\mathbf{W}$. A solution to this problem is the Cholesky decomposition [15], which requires the matrix $\mathbf{W}$ to be positive and definite. Hence, $\mathbf{C}$ is the Cholesky factorization of $\mathbf{W}$ satisfying (15).

The procedure for generating $\mathcal{L}$ correlated Rayleigh fading processes $z_\ell(t)$ $(\ell = 1, 2, \ldots, \mathcal{L})$ is summarized as follows. We first generate $\mathcal{L}$ uncorrelated complex Gaussian random processes $\mu_\ell(t)$ with the specified ACFs. Then, we determine the coloring matrix $\mathbf{C}$ from the desired correlation matrix $\mathbf{W}$ by applying the Cholesky decomposition. The resulting coloring matrix $\mathbf{C}$ is a lower triangular matrix such that $\mathbf{C}\mathbf{C}^T = \mathbf{W}$ holds. The correlated complex Gaussian random processes $y_\ell(t)$ $(\ell = 1, 2, \ldots, \mathcal{L})$ are obtained by a LT of $\mu_\ell(t)$, as shown in (7) or (8). At last, taking the magnitude of each $y_\ell(t)$ will result in the $\mathcal{L}$ desired cross-correlated Rayleigh fading processes $z_\ell(t)$.

III. Deterministic Simulation Model

In this section, an efficient deterministic SOS simulation model is presented. The generic procedure described in Section II will be followed here. According to [12, 16, 17], each of the $\mathcal{L}$ mutually uncorrelated complex Gaussian random processes can be modeled as:

$$\tilde{\mu}_\ell(t) = \tilde{\mu}_{1,\ell}(t) + j\tilde{\mu}_{2,\ell}(t) \tag{16}$$

where

$$\tilde{\mu}_{i,\ell}(t) = \sum_{n=1}^{N_{i,\ell}} c_{i,n,\ell} \cos(2\pi f_{i,n,\ell} t + \theta_{i,n,\ell}) \ , \quad i = 1, 2 \ . \tag{17}$$

Here, $N_{i,\ell}$ defines the number of sinusoids, mainly determining the realization expenditure and the performance of the channel simulator. In (17), $c_{i,n,\ell}$, $f_{i,n,\ell}$, and $\theta_{i,n,\ell}$ are called the Doppler coefficients, the discrete Doppler frequencies, and the Doppler phases, respectively. These simulation model parameters have to be determined in such a way that the statistical properties of the simulation model can approximate as close as possible the desired theoretical statistics. It is worth mentioning that the parameters $c_{i,n,\ell}$, $f_{i,n,\ell}$, and $\theta_{i,n,\ell}$ will be initialized during the simulation setup phase. Afterwards, they are known quantities and are kept constant during the whole simulation run phase. Consequently, $\tilde{\mu}_\ell(t)$ is a deterministic function and the resulting channel simulator is of deterministic nature. The ACF of $\tilde{\mu}_\ell(t)$ is given by

$$\tilde{r}_{\mu_\ell\mu_\ell}(\tau) = \sum_{i=1}^{2} \tilde{r}_{\mu_{i,\ell}\mu_{i,\ell}}(\tau) \tag{18}$$

where

$$\tilde{r}_{\mu_{i,\ell}\mu_{i,\ell}}(\tau) = \sum_{n=1}^{N_{i,\ell}} \frac{c_{i,n,\ell}^2}{2} \cos(2\pi f_{i,n,\ell}\tau) \ . \tag{19}$$

In order to ensure that $\tilde{r}_{\mu_{1,\ell}\mu_{2,\ell}}(\tau) = 0$ and $\tilde{r}_{\mu_\ell\mu_\lambda}(\tau) = 0$ for all $\ell, \lambda = 1, 2, \ldots, \mathcal{L}$ and $\ell \neq \lambda$, the following condition for the design of the discrete Doppler frequencies $f_{i,n,\ell}$ has to be fulfilled [12]

$$f_{i,n,\ell} \neq \pm f_{j,m,\lambda} \tag{20}$$

where $i, j = 1, 2$, $n = 1, 2, \ldots, N_{i,\ell}$, $m = 1, 2, \ldots, N_{j,\lambda}$, $i = j$ and $\ell = \lambda$ cannot hold at the same time. In [17], two parameter computation methods, namely, the method of exact Doppler spread (MEDS) and the L_p-norm method (LPNM), have been investigated in detail concerning how to satisfy the inequality (20). For completeness, these two methods are briefly reviewed in the following.

By using the MEDS [12], $c_{i,n,\ell}$ and $f_{i,n,\ell}$ are given by

$$c_{i,n,\ell} = \sigma_0 \sqrt{\frac{2}{N_{i,\ell}}} \tag{21}$$

and

$$f_{i,n,\ell} \ = \ f_{max} \sin\left[\frac{\pi}{2N_{i,\ell}}(n - \frac{1}{2})\right] \tag{22}$$

respectively, while $\theta_{i,n,\ell}$ are the outcomes of a random generator uniformly distributed over $(0, 2\pi]$. The condition (20) can be fulfilled if and only if the number of sinusoids $N_{i,\ell}$ are chosen in such a way that

$$\frac{N_{i,\ell}}{N_{j,\lambda}} \neq \frac{2n-1}{2m-1} \tag{23}$$

holds [17]. Note that relatively large values have to be chosen for $N_{i,\ell}$ when simulating more than 4 $(\mathcal{L} > 4)$ uncorrelated fading processes, which results in an inefficient implementation of the channel simulator. This disadvantage can be avoided if we replace $f_{i,n,\ell}$ by $f_{i,n,\ell} + \varepsilon$ when (23) is not fulfilled for only few pairs of (n, m) [17]. Here, ε is a very small random variable which guarantees that $f_{i,n,\ell} \neq \pm f_{j,m,\lambda}$ and $f_{i,n-1,\ell} < f_{i,n,\ell} + \varepsilon < f_{i,n+1,\ell}$ hold.

For the LPNM [12], $c_{i,n,\ell}$ and $\theta_{i,n,\ell}$ in (17) are the same as those given for the MEDS, while the quantities $f_{i,n,\ell}$ are determined by minimizing the following error norm

$$E^{(p)} \ = \ \left\{ \frac{1}{\tau_{max}} \int_0^{\tau_{max}} |r_{\mu_\ell\mu_\ell}(\tau) - \tilde{r}_{\mu_\ell\mu_\ell}(\tau)|^p d\tau \right\}^{1/p} \ , \quad p = 1, 2, \ldots \tag{24}$$

where τ_{max} defines an upper boundary value up to which the approximation of $r_{\mu_i\mu_\ell}(\tau)$ is of interest. An optimized set of discrete Doppler frequencies $f_{i.n.\ell}$ will be attained by applying a proper numerical optimization procedure. The inequality (20) can easily be satisfied by carrying out the optimization under any of the following four conditions [17]: 1) choosing $N_{i,\ell}$ such that the relation $N_{i,\ell} \neq N_{j,\lambda}$ holds. 2) minimizing (24) by using different values of p, 3) minimizing (24) with different values of τ_{max}, and 4) minimizing (24) by using different starting values for $f_{i.n,\ell}$.

Once multiple uncorrelated processes $\tilde{\mu}_\ell(t)$ are generated, the desired multiple cross-correlated processes $\tilde{y}_\ell(t)$ can be accomplished by a LT of $\tilde{\mu}_\ell(t)$ as follows

$$\tilde{\mathbf{Y}} = \mathbf{C}\tilde{\mathbf{U}} \tag{25}$$

where $\tilde{\mathbf{Y}} = [\tilde{y}_1(t) \quad \tilde{y}_2(t) \quad \cdots \quad \tilde{y}_{\mathcal{L}}(t)]^T$, $\tilde{\mathbf{U}} = [\tilde{\mu}_1(t) \quad \tilde{\mu}_2(t) \quad \cdots \quad \tilde{\mu}_{\mathcal{L}}(t)]^T$, and $\mathbf{C}$ is given by (9). It can easily be shown that the ACF of $\tilde{y}_\ell(t)$ and the CCF between $\tilde{y}_\ell(t)$ and $\tilde{y}_\lambda(t)$ $(\ell, \lambda = 1, 2, \cdots, \mathcal{L}$ and $\ell \neq \lambda)$ are given by

$$\tilde{r}_{y_\ell y_\ell}(\tau) = \sum_{k=1}^{\mathcal{L}} c_{\ell k}^2 \tilde{r}_{\mu_k\mu_k}(\tau) \tag{26}$$

and

$$\tilde{r}_{y_\ell y_\lambda}(\tau) = \sum_{k=1}^{\mathcal{L}} c_{\ell k} c_{\lambda k} \tilde{r}_{\mu_k\mu_k}(\tau) \tag{27}$$

respectively.

IV. Results and Discussion

In this section, we demonstrate the ability of the deterministic SOS channel modeling approach to accurately and efficiently simulate multiple cross-correlated Rayleigh fading processes. As an example, we consider the generation of $\mathcal{L}$ =3 fading processes with specified cross-correlation coefficients $\rho_{12} = 0.9$, $\rho_{13} = 0.8$, and $\rho_{23} = 0.6$ [5]. The resulting lower triangular coloring matrix $\mathbf{C}$ from the Cholesky decomposition of $\mathbf{W}$ is as follows:

$$\mathbf{C} = \begin{bmatrix} 1 & 0 & 0 \\ 0.9 & 0.4359 & 0 \\ 0.8 & -0.2753 & 0.5331 \end{bmatrix}. \tag{28}$$

Fig. 1 impressively illustrates the precise matching between the theoretical ACFs $r_{y_\ell y_\ell}(\tau)$ $(\ell = 1, 2, 3)$ and the approximate ACFs $\tilde{r}_{y_\ell y_\ell}(\tau)$ by using the MEDS and the LPNM. The numbers of sinusoids for the MEDS were chosen as follows: $N_{1,1} = 8$, $N_{2,1} = 9$, $N_{1,2} = 10$, $N_{2,2} = 12$, $N_{1,3} = 16$, and $N_{2,3} = 32$. For the LPNM, $N_{i,\ell} = 10$ was chosen for all $i = 1, 2$ and $\ell = 1, 2, 3$. The MEDS was employed to get the starting values of $f_{i.n,\ell}$. The upper limit for the integral in (24) was given by $\tau_{max} = 0.0549$ s. The optimization of the ACFs $\tilde{r}_{\mu_1\mu_1}(\tau)$, $\tilde{r}_{\mu_2\mu_2}(\tau)$, and $\tilde{r}_{\mu_3\mu_3}(\tau)$ was based on the error norms $E^{(p)}$ with $p = 1$, $p = 2$, and $p = 3$, respectively. For the LPNM, it is obvious that the ACFs $\tilde{r}_{y_\ell y_\ell}(\tau)$ are almost identical since $N_{i,\ell} = 10$ was chosen for all $i = 1, 2$ and $\ell = 1, 2, 3$. Due to the fact that different values of $N_{i,\ell}$ have to be selected when using the MEDS, the ACFs $\tilde{r}_{y_\ell y_\ell}(\tau)$ differ from each other. However, the performance of all $\tilde{r}_{y_\ell y_\ell}(\tau)$ $(\ell = 1, 2, 3)$ is determined by the smallest value of $N_{i,\ell}$, which is given by $N_{1,1} = 8$. Consequently, the LPNM provides a better approximation to $r_{y_\ell y_\ell}(\tau)$ than the MEDS for the given numbers of sinusoids. The CCFs of the reference model and the simulation model by using the MEDS and the LPNM are comparatively plotted in Fig. 2. Again,the LPNM has a better performance than the MEDS for the given numbers of sinusoids. It is important to mention that the approximation results of the ACFs and CCFs illustrated here are much better than those presented in [5].

Fig. 3 shows the simulated fading envelopes for three processes by using the LPNM with $\sigma_0^2 = 1/2$, $f_{max} = 91$, and $N_{i,\ell} = 10$. The envelopes are quite similar for the high correlation coefficient, while appear to be nearly uncorrelated for the low correlation coefficient. The corresponding simulated phase processes are presented in Fig. 4, demonstrating that the generated deep amplitude fades have corresponding hits in the phase process. This important property is a major concern of some applications such as fading channel equalizer design [18].

V. Conclusion

In this paper, it is shown how the deterministic SOS channel modeling approach can be applied for accurate and efficient simulation of multiple cross-correlated Rayleigh fading channels. The simulated processes have the attractive properties that their ACFs and CCFs perfectly match the desired ones. Also, our channel simulator can reproduce the important behavior that the phase changes markedly during deep fades. The described procedure will be useful for simulating, e.g., practical diversity channels, MIMO channels, and space-time-selective mobile fading channels.

References

[1] R.B. Ertel and H.H. Reed, "Generation of two equal power correlated Rayleigh fading envelopes," *IEEE Commun. Lett.*, vol. 2, no. 10, pp. 276–278, Oct. 1998.

[2] N.C. Beaulieu, "Generation of correlated Rayleigh fading envelopes," *IEEE Commun. Lett.*, vol. 3, no. 6, pp. 172–174, June 1999.

[3] A. Verschoor, A. Kegel, and J.C. Arnbak, "Hardware fading simulator for a number of narrowband channels with controllable mutual correlation," *Electron. Lett.*, vol. 24, no. 22, pp. 1367–1369, Oct. 1988.

[4] B. Natarajan, C.R. Nassar, and V. Chandrasekhar "Generation of correlated Rayleigh fading envelopes for spread spectrum applications," *IEEE Commun. Lett.*, vol. 4, no. 1, pp. 9–11, Jan. 2000.

[5] A. Hansson and T. Aulin, "Generation of n correlated Rayleigh fading processes for the simulation of space-time-selective radio channels," *Proc. European Wireless*, Munich, Germany, Oct. 6–8, 1999, pp. 269–272.

[6] N.C. Beaulieu and M.L. Merani, "Efficient simulation of correlated diversity channels," *Proc. IEEE WCNC'00*, Chicago, USA, Sept. 23–28, 2000, pp. 207–210.

[7] D.J. Young and N.C. Beaulieu, "The generation of correlated Rayleigh random variates by inverse discrete Fourier transform," *IEEE Trans. Commun.*, vol. 48, no. 7, pp. 1114–1127, July 2000.

[8] K.E. Baddour and N.C. Beaulieu, "Autoregressive models for fading channel simulation," *Proc. IEEE GLOBECOM'01*, San Antonio, USA, Nov. 25–29, 2001, pp. 1187–1192.

[9] S.O. Rice, "Mathematical analysis of random noise," *Bell Syst. Tech. J.*, vol. 23, pp. 282–332, July 1944.

[10] S.O. Rice, "Mathematical analysis of random noise," *Bell Syst. Tech. J.*, vol. 24, pp. 46–156, Jan. 1945.

[11] W.C. Jakes, Ed., *Microwave Mobile Communications*. New Jersey: IEEE Press, 1994.

[12] M. Pätzold, *Mobile Fading Channels*. Chichester: John Wiley & Sons, 2002.

[13] A. Leon-Garcia, *Probability and Random Processes for Electrical Engineering*. 2nd ed., New York: Addison-Wesley, 1994.

[14] R.H. Clarke, "A statistical theory of mobile-radio reception," *Bell Syst. Tech. J.*, vol. 47, pp. 957–1000, July/Aug. 1968.

[15] E. Kreyszig, *Advanced Engineering Mathematics*. 8th ed., New York: John Wiley & Sons, 1998.

[16] M. Pätzold, U. Killat, F. Laue, and Y. Li, "On the statistical properties of deterministic simulation models for mobile fading channels," *IEEE Trans. Veh. Technol.*, vol. 47, no. 1, pp. 254–269, Feb. 1998.

[17] C.X. Wang and M. Pätzold, "Methods of generating multiple uncorrelated Rayleigh fading processes," *Proc. IEEE VTC'03-Spring*, Jeju, Korea, Apr. 22–25, 2003, pp. 510–514.

[18] M. Fattouche and H. Zaghloul, "Equalization of $\pi/4$ offset DQPSK transmitted over flat fading channels," *Proc. IEEE ICC'92*, Chicago, USA, June 14–17, 1992, pp. 296–298.

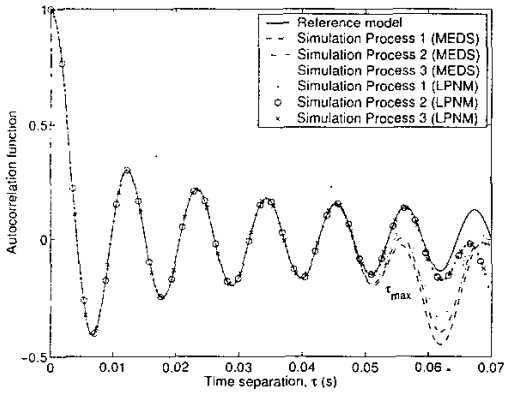

Fig. 1. The ACFs of the reference model and the simulation model by using the MEDS and the LPNM ($\sigma_0^2 = 1/2$, $f_{max} = 91$ Hz).

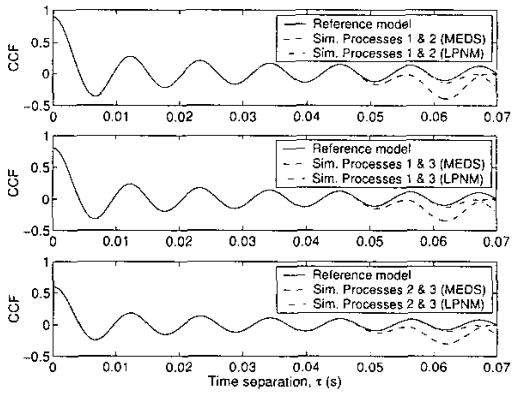

Fig. 2. The CCFs of the reference model and the simulation model by using the MEDS and the LPNM ($\sigma_0^2 = 1/2$, $f_{max} = 91$ Hz).

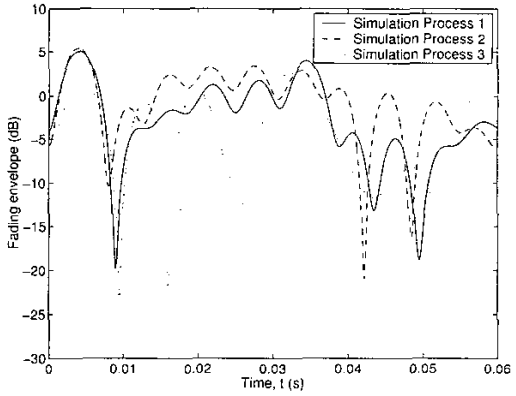

Fig. 3. Correlated fading envelopes by using the LPNM ($\sigma_0^2 = 1/2$, $f_{max} = 91$ Hz, $N_{i,\ell}$=10).

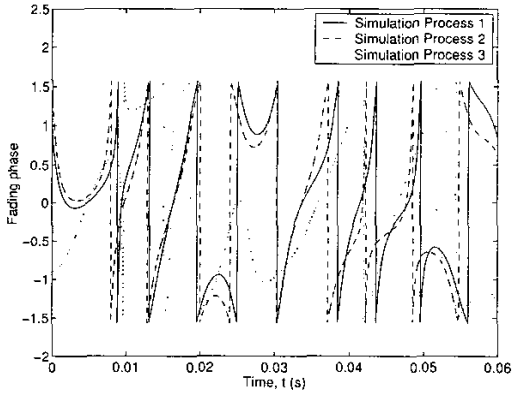

Fig. 4. Correlated fading phases by using the LPNM ($\sigma_0^2 = 1/2$, $f_{max} = 91$ Hz, $N_{i,\ell}$=10).